Subsea buoyancy gravity energy storage
an innovative modular solution for deepwater's applications

Novgorodcev, Andre R.; Jarquín-Laguna, Antonio

DOI
10.1049/icp.2023.1574

Publication date
2023

Document Version
Final published version

Published in
IET Conference Proceedings

SUBSEA BUOYANCY GRAVITY ENERGY STORAGE: AN INNOVATIVE MODULAR SOLUTION FOR DEEPWATER'S APPLICATIONS.

Andre R. Novgorodcev Jr.[1], Antonio Jarquín-Laguna[2]

[1] Offshore Engineering, Faculty of Civil Engineering and Geosciences, Delft University of Technology, the Netherlands
[2] Maritime and Transport Technology, Faculty of Mechanical, Maritime and Materials Engineering, Delft University of Technology, the Netherlands
**a.r.novgorodcevjunior@tudelft.nl*

Keywords: GRAVITY ENERGY STORAGE, BUOYANCY ENERGY STORAGE, SUBMERGED STORAGE SYSTEM, GRID STORAGE

Abstract

The increasing development of floating wind turbines has paved the way for exploiting offshore wind resources at locations with greater depth and energy potential. The study presents a novel Subsea Buoyancy Gravity Energy Storage System (SBGESS) that combines buoyancy energy storage and gravity energy storage technologies to overcome the intermittent nature of wind energy. The proposed system is assessed for time-shifting power delivery applications in two Brazilian offshore wind farm sites with varying wind conditions and water depths. The performance of the SBGESS is evaluated by considering different numbers of units, water depths, and control strategies. The results demonstrate that the SBGESS can effectively enhance offshore wind farms' capacity factor and power output during peak times, particularly in regions with lower wind potential and higher profundity.

1 Introduction

New technical developments and industrialisation of floating wind turbines will allow the construction of wind energy farms in regions with greater water depths (WD) and high-energy potential, reaching 15% of total installed capacity by 2050 [1]. Such wind farms could power electric grids or offshore Oil and Gas production systems, reducing greenhouse gas emissions. Energy storage solutions are essential for mitigating wind resources' intermittent nature in stand-alone and grid-connected applications. For stand-alone systems, given the variable supply and demand, the energy storage system (ESS) must be designed to ensure the power balance. Conversely, when connected to an electric grid, the system can serve various functions, ranging from frequency stability to seasonal balance. Moreover, the energy storage technology should be selected following the application requirements.

Among the available storage solutions, mechanical systems boast some of the highest roundtrip efficiencies, energy density, reliability, extended lifespans, and scalability [2]. Specifically, in the emerging field of offshore energy, buoyancy energy storage (ByES) and gravity energy storage (GES) technologies can capitalise on the deeper water environments, where substantial energy storage capacities can be achieved along the water column. GES employs submerged weights to store potential energy. While onshore developments have a few operational prototypes, scientific publications are scarce on offshore GES. The GES concept offers several advantages, such as theoretical roundtrip efficiencies of up to 90%, modularity, relatively low capital costs in the range of 50 to 100 USD/kW and up to 60 years of expected service life [2], [3]. By contrast, ByES harnesses buoyancy forces to store potential energy, functioning similarly to GES but in the opposite direction. ByES technology is even less explored in the literature, with only a few conceptual designs and preliminary lab scale tests. In those initial concepts, modelled blocks of floating materials like Styrofoam [4] or gas-filled vessels [5] were proposed to be used as floaters. The theoretical maximum roundtrip efficiency for ByES is reported to be 83%. The service life is similar to GES, and the capital costs are compatible with battery ESS (from 900 to 2000 USD/kW) [2]. Both technologies are suitable for applications that require up to 600 MW of power output and 1 GWh of energy storage [2].

Considering these favourable characteristics, a new concept combining the two technologies mentioned above, called Subsea Buoyancy Gravity Energy Storage System (SBGESS), was proposed to operate in a stand-alone subsea water injection system powered by two 12 MW floating wind turbines to be installed at an ultradeep water (up to 3000 m) oil field in Brazil [6]. The system was dimensioned to increase the annual water injection volume while reducing the number of stops to avoid premature failures of the pumps.

A cluster of SBGESS installed in high water depths could attend to energy storage capacity (ESC) and power output requirements to deal with the daily mismatches between the supply of an offshore wind park and the grid demand for

https://doi.org/10.1049/icp.2023.1574

electricity, called time-shifting energy storage. The adoption of this kind of storage is essential to reduce the curtailment, the cycling of baseload generation and the operation of high-cost and high-emitting peaking power plants, allowing an increase in the variable renewable energy sources [7].

The present study aim to evaluate the application of a cluster of SBGESS systems directly connected to two 1GW floating offshore wind farms in two distinct locations for time-shifting power delivery. The influence of the water depth, number of units and control strategy over the energy exported during peak time is evaluated. Even though economic aspects are important, these are not evaluated as the development is in the initial phase, and there are some uncertainties regarding the electrical components and installation costs.

1.1 Subsea Buoyancy Gravity Energy Storage System

An artistic impression of the SBGESS is depicted in Figure 1. In this concept, drum hoists mounted on a semi-sub structure (in red) lift concrete cylinders (in blue) to tore gravitational potential energy, which can be released by inverting the electric motor's operation. Simultaneously, light floaters (in green) are deepened or lifted with similar forces in opposite directions, maintaining the platform's stability while storing or releasing buoyancy potential energy. The rated power of each component is obtained by multiplying the resultant vertical force on the direction of the movement by the rated velocity. There are three forces terms to be considered the weight, the buoyancy and the fluid resistance (drag) that opposes the movement.

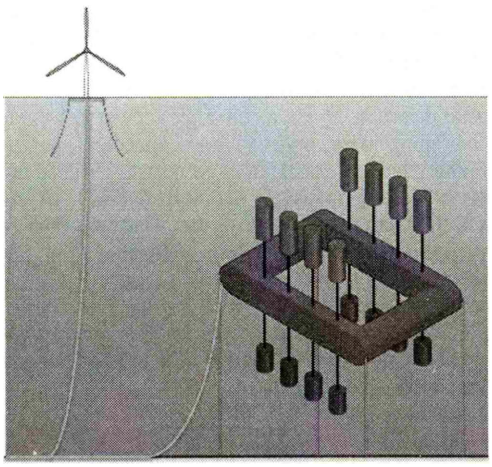

Figure 1. Subsea Buoyancy Gravity Energy Storage System (SBGESS), an artistic impression.

Each set of gravity and buoyancy unit is called an energy storage module (ESM) and can operate separately or together with other modules according to the power demand. The vertical velocity in each ESM could also change to adjust the power input and output but is limited to the rated velocity presented in Table 1 to reduce the power losses due to drag forces, which is proportional to v^3. The configuration with multiple ESM allows the control system to compensate for the reduction in the power output due to the deceleration of the blocks when closing to the end of its travel by initiating the acceleration of the elements of other ESM. The SBGESS receives power from a grid or a wind park substation through an alternate current (AC) link. The discharge can be made through the same link or directly to an end consumer, depending on the application. An energy conversion module i respon ible for the transformation of power to and from the winch's electric motors, guided by the control strategy put in place by the central control unit.

The semi-submerged configuration keeps the surface clear for navigation and reduces the influence of waves and superficial currents on the dynamics of the energy storage system avoiding collisions between the elements and reducing the loads on the mooring system. Another advantage is that the weights do not reach the seabed or interfere with cables, oil risers and other submerged structures in the installation area. Other concepts [3], [8] utilise multiple weights or floaters per winch, requiring remote-operated robots to connect and disconnect and a storage area with a significant relative motion relative to the platform. The SBGESS keeps the weights and floaters connected to avoid such problematic operations, especially with strong sea currents or waves, and to waive the use of active ballast control.

The initial dimensions of the SBGESS are similar to the ones of the buoy support riser successfully installed in the Santos Basin offshore Brazil at 2140 m depth [9]. This configuration allows the installation of 2 rows of ESMs, one on each side of the structure, totalising eight modules. The SBGESS also shares the same tension-leg platform (TLP) configuration, where pre-tensioned tendons installed in each of the structure's corners are connected to torpedo anchors. The type of concrete was changed since [6], resulting in the following dimensions and energy storage parameters:

Table 1. SBGESS main dimensions and rated parameters.

Parameter	SBGESS	weights	floaters
Length [m]	55		
Width/Radius [m]	40	2.5	2.5
Height [m]	10	7.3	12.3
Number of units		8	8
Rated velocity [m/s]		1	1
Total mass [t]	2800	3078	96.4
Rated power [MW]	37.16	2.32	2.32
ESC [MWh]:			
• At 1000m WD	5.16	2.58	2.58
• At 2000m WD	10.32	5.16	5.16

1.2 Case Study for the Brazilian Coast

Brazil has more than 32 GW of onshore wind farms occupying the sixth position in the global ranking of installed capacity [10]. Despite representing 13% of the national electric installed capacity, no offshore wind project was implemented in Brazil when writing the present manuscript. However, the situation might change soon as 74 projects, totalling 182 GW, are waiting for preliminary environmental approval, according to IBAMA (the Brazilian Institute for the Environment and Renewable Natural Resources) [11].

The proposed offshore wind projects are distributed into five regions as re ented in Figure 2. Regions one, two, three and five are regions with high wind potential, reaching an annual average wind velocity of 10 m/s at 150 m in some sites [12]. In region five, the annual average wind peeds are below 9 m/s, but this region is closer to the heavy energy con umers, reducing the transmis ion cost and losses. Another advantage of region five is that it is close to the leading offshore oil production sites and can take advantage of the local port and industrial infrastructure. The bathymetry in these regions [11] wa evaluated, and two sites near operational offshore oil fields, called RN (4.75°S, 36.5°W) and Libra (24.5°S, 42.5°W), with different wind potential and water depth, were selected.

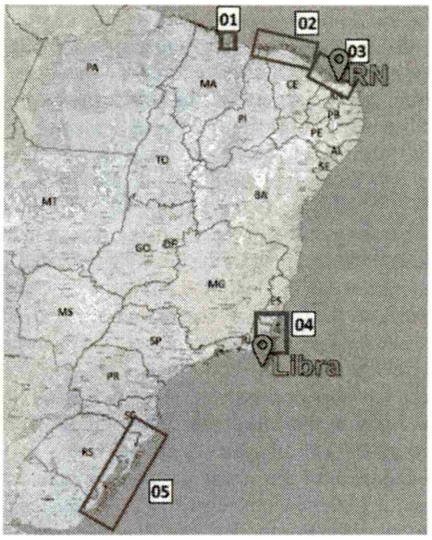

Figure 2. Map of the offshore wind projects that have requested preliminary environmental approval in Brazil and the location of the study sites adapted from [11].

RN site is positioned inside region three on the coast of Rio Grande do Norte (RN) state. The location has high wind potential (average wind speed of 9.4 ± 2.5 m/s), as shown in the result section. The maximum water depth of the park s location is 200 m, but it is on the edge of a slope that reaches more than 2000 m WD in 20 km. Libra site is located in the oil field of the same name in Santos Basin, with recoverable resources between 7.9 and 15 billion barrels of oil [13], where offshore wind power could support the electrification of offshore oil platforms that usually burn up to 5% of the oil and gas production to energise the internal processes [14]. Two examples of such application are the Hywind Tampen project in Norway [15] and the pilot project at the Wenchang oilfield in China [16].

A floating wind farm in the Libra field could also be connected to the national grid to increase the platform's energ supply reliability and surplus power export. Eventually, the park could commercialise all the power as the oil production fade. The average wind speed is smaller, and the standard deviation is higher (8.2 ± 3.6 m/s) than the one of the RN, but Libra has the advantage of being in ultra-deep waters, greater than 2000 m, increasing the energy storage capacity of the SBGESS.

According to a normative resolution 1000/2001 from the Brazilian National Energy Agency (ANEEL) [17], Brazil's electrical tariffs are divided into three tariff stations according to demand. The peak time i a three-hour period during workdays with maximum electrical load in a distribution area. The intermediate consists of one hour before and one hour after the peak and is a transition for the out-of-peak period that corresponds to the remaining hour of the day. The peak time changes according to the distribution network and may start at 17:00, 17:30 and 18:00 [18]. The Brazilian ational Grid Operator (ONS) divides the day into three periods to study the impact of wind and solar source on the transmission line [19]. The light period is between 0:00 to 07:00, the heavy period is from 18:00 to 21:59, and the re t of the day is the average period. In the present work, the daily peak time would be considered from 18:00 to 20:59, and the light period according to O S, will be adopted as the standard charging period.

2 Methodology

The following simulation methodology shown in Figure 3 is proposed to evaluate the performance of the SBGESS as a daily power peak shaver operation on the selected sites. The time domain simulations of the system and the results processing are performed in a computational model developed for the current project in Python.

Figure 3. Computational model flowchart

The first step is to generate a synthetic power output of a wind park installed in the interest regions combining a reanalysis of hourly wind data and the power curve of the selected turbine model. The resulting power is combined with the parameters of the energy storage system and the control strategy to simulate the hourly power output with energy storage for each park. A sensitivity analysis is done by changing the number of SBGESS units (50 to 200) and the water depth (500 to 2000 m). Moreover, the influence of the charging time duration i evaluated by adju ting the control strategy. Finally, the resulting peak time power outputs are compared with the different energy storage parameter and the output in the same period without energy storage.

2.1 The power output of the wind park

Reanalysis of the wind data for the central positions of RN and Libra sites was obtained from the Copernicus climate data project. For convenience, the selected wind parks central position coincides with the Copernicus nodes' position, eliminating the need for interpolation. The data consists of hourly wind speed values at 100 m height over 43 year (1979 – 2022) using reanalysi models [20].

The projects awaiting environmental approval in Brazil utilise turbines of at least 12 MW [11]. Considering the additional structural challenges of floating platforms, a commercial 12 MW offshore wind turbine was selected to power both parks. The hourly power output of the park is calculated by combining the wind output with the turbine's power curve [21]. The proposed wind parks will have 84 turbines, totalising 1008 MW. For the sake of simplicity and as the work is focused on the energy storage system, wake effects and other farm aspects that reduce the power output of the park are not considered in the present work.

2.2 SBGESS power and energy storage capacity

The energy storage capacity of each SBGESS is a function of the number of installed modules (N), the rated power output of each ESM (P) and the operational time, which is defined by the length of the cables (L) and the maximum charging and discharging velocities (v). Considering that N_{SBGESS} is the number of SBGESS installed, and the total energy storage capacity (ESC_T) is given by:

$$ESC_T = N_{SBGESS}\, P\, N\, \frac{L}{v} \tag{1}$$

For grid scale time-shifting power delivery applications, the eight modules of each SBGESS will operate in parallel (N=8), generating eight times the power of each separate module. The power output of the wind park substation to charge each SBGESS with the rated power (P_{charge}) and the power delivered at the same point ($P_{discharge}$) are:

$$P_{charge} = \frac{NP}{\sqrt[2]{\eta_{ES}\, \eta_{Tr}}} \tag{2}$$

$$P_{discharge} = N\, P\, \sqrt[2]{\eta_{ES}\, \eta_{Tr}} \tag{3}$$

where η_{ES} is the roundtrip energy storage efficiency, and η_{Tr} is the transmission efficiency. According to [3], the roundtrip efficiency considering the electrical and mechanical components losses of a GES concept with dimensions and mass in the same order of magnitude could be estimated at 0.90, and the drag losses for speeds in the order of 1 m/s are negligible. In contrast, [5] estimate the roundtrip efficiency of a ByES system with a similar Reynolds number, an additional pulley system and multiple floaters mounted vertically in 0.83. The present work adopts a conservative η_{ES} of 0,83, considering that the losses are equally distributed in the charging and discharging process. The length of the transmission cables connecting the wind park substation and the energy storage is assumed to be 1 km in the present development phase, where the site layout is not defined. For such distance and power level, three-core MVAC cables are the standard option adopted by the offshore wind industry [22], considering that the system operates at rated power, resulting in η_{Tr} = 0.975.

Considering the efficiencies, P_{charge}= 41.35 MW and $P_{discharge}$ = 32.46 MW. It is interesting to notice that 31 SBGESS are sufficient to provide the power output of the wind park, with the number of units defined by the ESC_T instead of the power output.

2.3 Control strategy

Two control strategies are adopted in the current project, and both discharge the stored energy during the peak demand time to complement the power output of the wind park. The objective is to export the nominal power of the park. In the standard mode (std), energy is stored daily during the small energy consumption period from midnight until 7:00 hrs and discharges the energy at peak time, reducing the curtailment during the low consumption period and increasing the operation at nominal power during peak time. The energy output of the park may not be enough to charge the energy storage system, mainly from February to June when the winds are weaker. An extended charging time mode (ex) could be adopted to maximise the power output during peak time by charging the SBGESS from midnight until 17:00 hrs.

During the charge period, the computational model evaluates the available energy storage capacity and redirects the maximum power output of the wind park to charge the SBGESS units, prioritising the partially loaded ones. During peak time, the model checks the charging state to evaluate the number of charged SBGESS modules and define the maximum available discharge power to complement the exported energy. All this operation is repeated in one-hour periods, as the initial input is the hourly wind data. An example of an operation day is illustrated in Figure 4, where the green line represents the hourly power output of the wind park, and the blue and orange solid lines represent the power output with the energy storage for both strategies. The traced lines represent the charging state (CS) of the SBGESS. On that particular day in the Libra site, the SBGESS with 100 units installed at 2000 m of water depth starts the day with zero energy and uses all the power generated by the wind park to charge until 7:00, when the charging state reaches 0.88 for the standard strategy. For the EX, the charging continues for one more hour before it reaches full charge. The stored energy is then used to complement the power output of the wind park to its full power during peak time. After the peak time, the CS is 0.11 and 0.23 according to the strategy, and a new charging cycle starts at midnight (00:00).

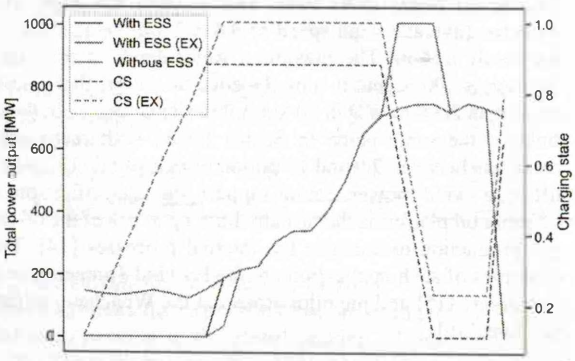

Figure 4. Total power output with and without energy storage and charging state with standard and extended (EX) control strategy for the Libra site with 100 SBGESS at 2000 m WD.

3 Results and discussion

The average wind velocities in the RN and Libra sites are lower between February and June (respectively 8.0 m/s and 7.4 m/s versus 10.3 m/s and 8.7 m/s in the rest of the year), reducing the park's power output, as seen in Figure 5. In this figure, the blue lines represent the average power generated during the indicated month without energy storage. The other lines indicate the increase in the power obtained with the adoption of 100 SBGESS installed at 1000 and 2000 m water depths. The ESC_T is indicated between the parenthesis on the legend.

The Libra site has a lower wind power output over the year and obtained a maximum average power of 607 MW in September and a minimum of 340 MW in April. The power production reaches zero on some days in this site from February to June due to the reduced wind. Adding 100 SBGESS at 2000 m of water depth increases the maximum average power output to 741 MW and the minimum to 516 MW.

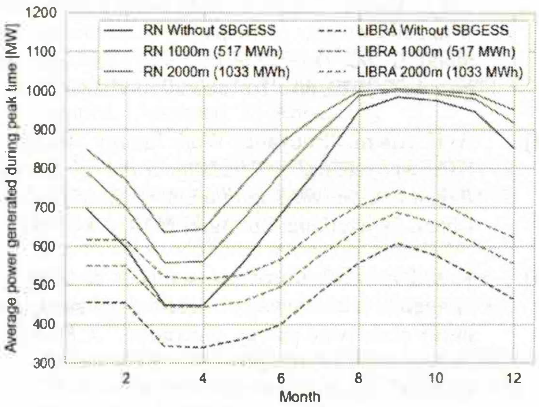

Figure 5. Average power during peak time along the year without energy storage and 100 SBGESS units installed in different water depths for the selected sites.

In contrast, the wind park in RN could provide up to 982 MW on average for the maximum production month, almost the rated power of the park, indicating that there is small space to increase the output for these months with the addition of energy storage systems. The advantage of adopting the SBGESS appears in the months with less wind, mainly March and April, when the average power is increased from 448 MW to 635 and 643 MW, respectively. Notably, the Libra wind farm will be installed in a region with more than 2000 m of water column, while the RN site has a water depth range from 200 to 1000 m within 10 km, which can extend to 2000 m at double that distance. Thus, if comparing the performance of the ESS in the park with lower potential but double water depth, the power difference in the low wind period is reduced to 40 MW.

Another way to analyse the influence of the number of units and water depth on the park's performance is to look at the capacity factors during daily peak time. The capacity factor is defined as the ratio of the net electricity generated, for the time considered, to the energy that could have been generated at full-power operation during the same period [23], that, in our case, is the daily period between 18:00 and 20:59.

Figure 6 shows the capacity factor analysis for the Libra site, with the trace dot black line representing the capacity factor without energy storage, the solid lines representing the field's capacity using the standard control strategy, and the dashed lines representing the extended charging time strategy. Adopting only a fifth of the energy storage units charging during the low consumption period provides a 6% increase in capacity factor. Adopting an extended charging period brings reduced benefits because the system is usually fully charged with the original strategy. Increasing the water depth increases the ESC_T almost linearly but without reflecting integrally in the capacity factor during peak time, as the power provided by the wind park is insufficient to reach a complete charge. The extended charging mode led to an additional increase in the capacity by up to 4% in the cases with 150 and 200 SBGESS, reaching 72 and 79%, respectively.

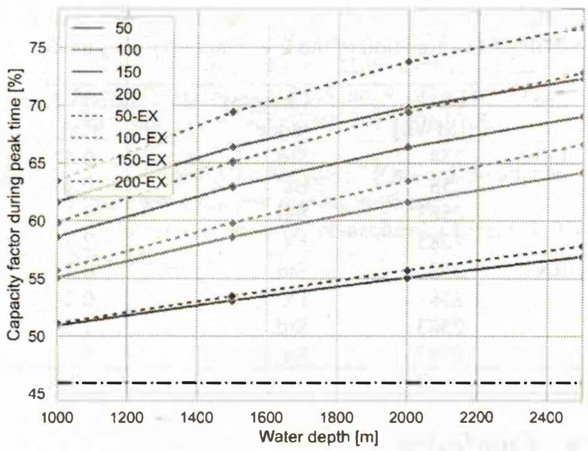

Figure 6. Capacity factor during peak time in the Libra site as a function of water depth for different number of SBGESS with standard and extended (EX) control strategy.

The influence of the extended charging mode is less significant for the RN site as the power output of the park leads to an improved charging state of the batteries. The higher charge state, combined with the reduced power demand from the batteries, enables the achievement of up to 91% capacity factors. The maximum capacity factor increases by using the extended charge for this site is 1%, as seen in Figure 7.

One of the advantages of the SBGESS over thermal and chemical energy storage is that it retains the charge independently of the storage time. The energy lost in the Libra site is higher than in the RN, as it is subjected to deeper discharge cycles. A similar increase in energy loss appears for the extended charge mode, as seen in Table 2.

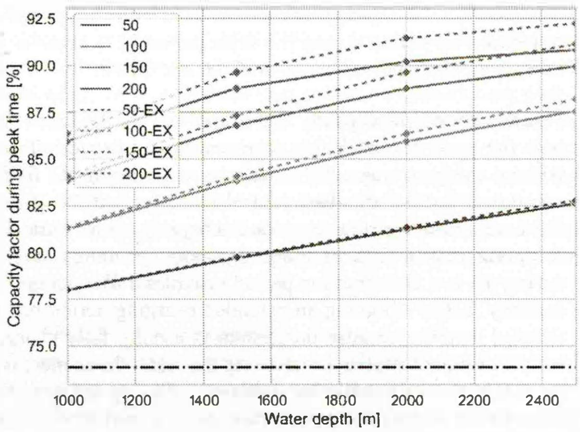

Figure 7. Capacity factor during peak time in the RN site as a water depth function for different SBGESS with standard and extended (EX) control strategy.

Table 2. Percentage of the generated energy lost in the SBGESS as a function of the ESC_T and Charging mode.

Site	ESC_T [MWh]	Charging mode	Energy loss [%]
Libra	258	Std.	0.4
	258	Ex	0.4
	2583	Std.	2.1
	2583	Ex	2.5
RN	258	Std.	0.2
	258	Ex	0.2
	2583	Std.	1.0
	2583	Ex	1.1

4 Conclusion

The present study addressed the application of a Subsea Buoyancy Gravity Energy Storage System (SBGESS) for time-shifting power delivery in floating offshore wind parks in Brazil. The system's performance was evaluated in two offshore sites with different wind conditions and water depths. The analysis showed that SBGESS could significantly improve the capacity factor and power output during peak times, particularly in areas with lower wind potential. The system proved particularly effective in regions with higher water depth, as the energy storage capacity scales linearly with the available displacement of the floats and weights. At the same time, the costs exhibit a marginal escalation, as only the mooring system and the length of the traction cables need to be increased.

For the Libra site, the capacity factor increased by up to 6% when adopting 50 SBGESS units and 26% with 200 units. In the RN site, where a higher capacity factor of 74% at peak time without energy storage was found, the capacity factor could still reach values up to 92%. The extended charging mode further increased the capacity factor for the Libra site by 4%, but it had a less significant impact on the RN site. In summary, the results highlight the potential of the proposed SBGESS as an effective energy storage solution for deep water offshore wind farms, contributing to daily time-shifting power delivery and enhancing the system's overall performance.

5 Acknowledgements

The authors would like to thank PETROBRAS, Brazil, for supporting the development of the SBGESS system.

6 References

[1] DNV, "Floating wind: Turning Ambition into Action," Report, 2023.

[2] Z. Wang, R. Carriveau, D. S. -K. Ting, W. Xiong, and Z. Wang, "A review of marine renewable energy storage," *Int. J. Energy Res.*, vol. 43, no. September 2018, pp. 6108–6150, 2019, doi: 10.1002/er.4444.

[3] J. F. Toubeau, C. Ponsart, C. Stevens, Z. De Grève, and F. Vallée, "Sizing of underwater gravity storage with solid weights participating in electricity markets," *Int. Trans. Electr. Energy Syst.*, no. June, pp. 1–17, 2020, doi: 10.1002/2050-7038.12549.

[4] A. H. Alami, "Buoyancy Work Energy Storage (BAES) Systems," in *Mechanical Energy Storage for Renewable and Sustainable Energy Resources*, Cham, Switzerland: Springer, 2020, pp. 87–92.

[5] K. P. Bassett, R. Carriveau, and D. S. K. Ting, "Integration of buoyancy-based energy storage with utility scale wind energy generation," *J. Energy Storage*, vol. 14, pp. 256–263, 2017, doi: 10.1016/j.est.2017.04.013.

[6] A. R. Novgorodcev Jr., F. Mols, and A. Jarquín Laguna, "Subsea buoyancy and gravity energy storage system for deep-water applications: a preliminary assessment," in *Proceedings of the ASME 2022 41st International Conference on Ocean, Offshore and Arctic Engineering - OMAE 2022*, 2022.

[7] A. B. Gallo, J. R. Simões-Moreira, H. K. M. Costa, M. M. Santos, and E. Moutinho dos Santos, "Energy storage in the energy transition context: A technology review," *Renew. Sustain. Energy Rev.*, vol. 65, pp. 800–822, Nov. 2016, doi: 10.1016/J.RSER.2016.07.028.

[8] L. B. Luo Z, Tian Y, Huang L, Yang F, "A gravity energy storage system using ocean depth difference," CN103867409B, 2016.

[9] I. Cruz *et al.*, "The new technology enablers developed and deployed on a live project," in *Offshore Technology Conference 2015*, 2015, vol. 3, pp. 2033–2046, doi: 10.4043/25832-ms.

[10] ABEEOLICA, "Infowind #30," Report, Feb-2023.

[11] IBAMA, "Complexos eólicos offshore - projetos com processos de licenciamento ambiental abertos no IBAMA," Map, 2023. [Online]. Available: https://www.gov.br/ibama/pt-br/assuntos/laf/consultas/mapas-de-projetos-em-licenciamento-complexos-eolicos-offshore. [Accessed: 14-Apr-2023].

[12] R. Dutra *et al.*, "Atlas do Potencial Eólico Brasileiro - 2nd Edition," *CEPEL - Cent. Pesqui. Energ. Elétrica*, p. 50, 2017.

[13] Offshore Technology, "Libra Oil Field, Santos Basin." [Online]. Available: https://www.offshore-technology.com/projects/libra-oil-field-santos-basin/. [Accessed: 15-May-2023].

[14] Wood Mackenzie, "Why powering oil and gas platforms with renewables makes sense," Report, 2019.

[15] Equinor, "Hywind Tampen," 2023. [Online]. Available: https://www.equinor.com/energy/hywind-tampen. [Accessed: 23-Apr-2023].

[16] A. Buljan, "China Connects Deepwater Floating Wind Platform to Wenchang Oilfield | Offshore Wind." [Online]. Available: https://www.offshorewind.biz/2023/05/22/china-connects-deepwater-floating-wind-platform-to-wenchang-oil-field/. [Accessed: 23-May-2023].

[17] Agência Nacional de Energia Elétrica – ANEEL, "Resolução Normativa ANEEL N° 1.000, de 7 de Dezembro de 2021(*)," 2021.

[18] G. Rocha and R. Resende, "Conheça os horários de ponta no consumo de energia no seu estado," *Solar Volt Energy*. [Online]. Available: https://www.solarvoltenergia.com.br/blog/tudo-sobre-os-horarios-de-ponta-no-consumo-de-energia/. [Accessed: 01-Apr-2023].

[19] Operador Nacional do Sistema Elétrico - ONS, "Histórico da Geração Eólica e Fotovoltaica." [Online]. Available: https://www.ons.org.br/paginas/resultados-da-operacao/historico-da-operacao/dados-de-geração-eólica-e-solar. [Accessed: 01-Apr-2023].

[20] H. Hersbach *et al.*, "The ERA5 global reanalysis," *Q. J. R. Meteorol. Soc.*, vol. 146, no. 730, pp. 1999–2049, Jul. 2020, doi: 10.1002/QJ.3803.

[21] EÓLICA BRASIL LTDA, "Relatório de produção energética - Certificação de medições anemométricas e de produção de energia," Ceará - Brazil, 2019.

[22] A. Madariaga, J. L. Martín, I. Zamora, S. Ceballos, and O. Anaya-Lara, "Effective assessment of electric power losses in three-core XLPE cables," *IEEE Trans. Power Syst.*, vol. 28, no. 4, pp. 4488–4495, 2013, doi: 10.1109/TPWRS.2013.2263514.

[23] NRC, "Capacity Factor (net)." [Online]. Available: https://www.nrc.gov/reading-rm/basic-ref/glossary/capacity-factor-net.html. [Accessed: 01-May-2023].